Quantitative characterization of the water trimer torsional manifold by terahertz laser spectroscopy and theoretical analysis. II. $(H_2O)_3$

Mac G. Brown,[a] Mark R. Viant,[b] Ryan P. McLaughlin,[c] Christy J. Keoshian, Ernest Michael, Jeff D. Cruzan,[d] and Richard J. Saykally[e]
Department of Chemistry, University of California, Berkeley, California 94720

Ad van der Avoird[f]
Institute of Theoretical Chemistry, NSR-Center, University of Nijmegen, Toernooiveld, 6525 ED Nijmegen, The Netherlands

(Received 19 May 1999; accepted 4 August 1999)

We report the measurement of two new $(H_2O)_3$ bands by terahertz laser vibration–rotation–tunneling (VRT) spectroscopy. Both bands have been assigned to torsional (''pseudorotational'') transitions and are highly perturbed by Coriolis interactions. The $42.9\,cm^{-1}$ band corresponds to the $k=\pm2\leftarrow\pm1$ transition while the $65.6\,cm^{-1}$ band corresponds to the $k=\pm2\leftarrow0$ transition. A model Hamiltonian is derived which allowed a global fit of 361 VRT transitions of these two new bands and the previously reported torsional band at $87.1\,cm^{-1}$. Each of the bifurcation tunneling components is accurately described. This global fit represents a complete description of the VRT transitions of $(H_2O)_3$ up to $150\,cm^{-1}$, and complements our similar treatment of the $(D_2O)_3$ torsional dynamics. © *1999 American Institute of Physics.* [S0021-9606(99)00341-4]

I. INTRODUCTION

Since the experimental characterization of the water trimer in 1992 with terahertz VRT spectroscopy,[1] a great deal of experimental and theoretical results have been realized for this complex. Four additional torsional bands of $(D_2O)_3$ have been added to the first observation,[2–4] which, along with the development of a detailed model Hamiltonian, have allowed a complete fit[2] of the torsional manifold of $(D_2O)_3$ up to energies near $100\,cm^{-1}$. Many calculations have been performed on the $(D_2O)_3$, $(H_2O)_3$, and mixed isotope forms of the water trimer in order to theoretically describe this manifold of states.[5–18] A direct comparison between the theory and experiment has been possible for $(D_2O)_3$ due to the large number of precisely measured torsional vibrations. The same has not been true for $(H_2O)_3$ where, prior to the present study, only a single torsional vibration had been observed.[3] It is important to achieve a quantitative description of these torsional states for both $(H_2O)_3$ and $(D_2O)_3$ because such results will facilitate a determination of the complex three-body contributions to the water force field, in conjunction with our efforts toward a spectroscopically accurate description of the water pair potential.[19]

The minimum energy structure of the water trimer, the asymmetric homodromic (C_1) ring, see Fig. 1, has been established by many *ab initio* calculations.[20–23] It is a classic example of a frustrated equilibrium. Two nonbonded (''free'') hydrogens are on the same side of the oxygen plane, sterically interacting. Experimentally it has been demonstrated that this nonplanar asymmetric structure vibrationally averages to a planar symmetric top via the torsional (flipping) motion,[1,3] illustrated in Fig. 1. This large amplitude hydrogen torsional motion creates a very low barrier degenerate rearrangement process, a rearrangement mechanism predicted as early as 1975 by Owicki, Shipman, and Scheraga.[24] The torsional quantum levels of the water trimer have been considered at various levels of theory. The first, and simplest, was a one-dimensional treatment by Schütz *et al.*, who used an adjustable cosine wave as the potential.[17,18] Their calculation obtained the correct ordering of the energy levels but gave poor quantitative results. A Hückel treatment of the water trimer by Wales[16] gave an improved description of the energy level structure but required fitting a tunneling parameter (β_1) to the experimental data. A pair of model torsional potential energy surfaces fit to *ab initio* calculated points were created by Bürgi, Graf, Leutwyler, and Klopper (the BGLK potential),[10] and by van Duijneveldt-van de Rijdt and van Duijneveldt[14] (the DD potential). Several more advanced dynamics calculations have been performed on these potentials including two-dimensional[12] and three-dimensional calculations excluding rotation[13] and, most recently, three-dimensional calculations by van der Avoird *et al.*[6,7] that couple the torsional motion to the overall rotation of the trimer complex.

The second type of internal large amplitude motion in the water trimer is bifurcation tunneling (for which one has also used the less descriptive term ''donor tunneling''). This is a rearrangement process wherein a single water monomer exchanges its hydrogen bonded and free hydrogen atoms by tunneling through a bifurcated transition state, as shown in Fig. 2. It could be observed experimentally[3] and unambigu-

[a]Present address: Department of Chemistry, University of Oregon.
[b]Present address: Department of Animal Science, University of California, Davis, CA 95616.
[c]Present address: Department of Chemistry, University of Washington.
[d]Present address: Department of Molecular and Cellular Biology, Harvard University, Cambridge, MA 02138.
[e]Author to whom all correspondence should be addressed.
[f]Electronic mail: avda@theochem.kun.nl

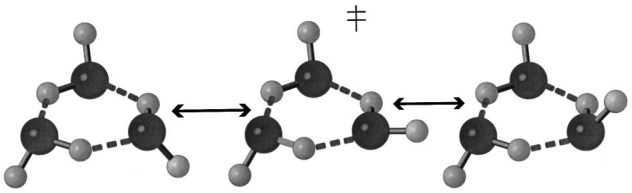

FIG. 1. The equilibrium structure of the water trimer is a near-oblate asymmetric top. Torsion of the free hydrogens approximately about the hydrogen bonds is the dominant low-frequency motion of this trimer. This low barrier rearrangement process involves the motion of a free hydrogen from one side of the O–O–O plane to the other (''flipping'') and is predicted to have a $90\,cm^{-1}$ barrier (Ref. 20). As a result each free hydrogen spends an equal amount of time above and below the O–O–O plane, thus vibrationally averaging the asymmetric (C_1) equilibrium structure to that of an oblate symmetric top in the ground state. The O–O bond distance has been determined as 2.84 Å through a simple model calculation based on the spectroscopic data (Ref. 36). Each of the VRT bands reported in this work arises from the manifold of states created through this torsional vibration.

ously identified, since it gives rise to a splitting of the torsional levels and transitions into quartets. The splitting between the lines in these quartets, typically about 300 MHz for $(H_2O)_3$ and about 5 MHz for $(D_2O)_3$, is much smaller than the energy gaps between the torsional levels. This is because the corresponding barrier height, calculated by Fowler and Schaefer[20] as $525\,cm^{-1}$ (corrected for zero point effects), is substantially higher than the torsional barrier.

The collection and analysis of experimental data for the torsional level manifold of $(H_2O)_3$, including the rotational structure and bifurcation splittings of these levels, has lagged far behind that accumulated for $(D_2O)_3$. The parallel band at $87.1\,cm^{-1}$ is the only measurement that has been reported previously.[3] Here we report the observation of two new torsional bands of $(H_2O)_3$ as well as the derivation of a model Hamiltonian used in a global fit of all three bands, thus completely characterizing the torsional manifold of $(H_2O)_3$ up to energies of $150\,cm^{-1}$.

II. THEORY

A. Torsion and bifurcation tunneling

The construction of the torsional manifold for the water trimer, including a group theoretical treatment, has been detailed in several previous papers.[3,6,7,16,25] Also the bifurcation tunneling splitting of the levels was considered in these references. In light of the fact that this paper represents the first experimental determination of the torsional energy level manifold for $(H_2O)_3$ we review here the basic theory behind the torsional and bifurcation tunneling dynamics in the water trimer.

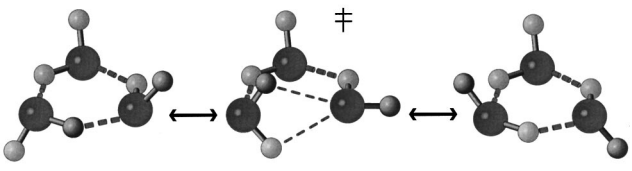

FIG. 2. A higher barrier rearrangement process observed for the water trimer is bifurcation tunneling, where the roles of the free and bound hydrogens of a water in the cluster are switched. The pathway for this process is predicted to traverse a bifurcated transition state. This rearrangement gives rise to the quartet tunneling splitting observed for each torsional band of $(H_2O)_3$ and $(D_2O)_3$. Notice that an adjacent water molecule flips as part of the tunneling pathway. A previous group theoretical analysis (Refs. 6 and 7) suggests that this pathway, rather than an independent C_2 rotation of the water monomer, is evidenced in our spectra.

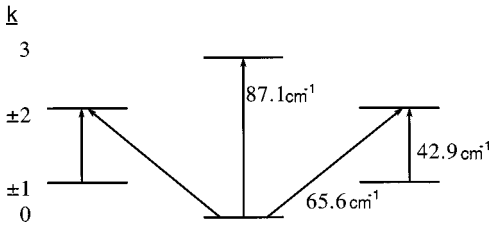

FIG. 3. The lowest four torsional energy levels ($k=0,\pm1,\pm2,3$) along with the allowed transitions and the observed frequencies. Symmetry restrictions allow only transitions with $\Delta(k-K)=3$ (modulo 6) to be observed, as explained in the text. Between the highest ($k=3$) level in this figure and the next higher (also $k=3$) level is a large energy gap. The next higher ($k=3 \leftarrow \pm1$) transition is expected at $\approx 170\,cm^{-1}$, presently out of the range of our spectrometer.

The equilibrium structure of the water trimer may interconvert between six of the 96 equivalent minima covering the 12-dimensional intermolecular potential energy surface (IPS) through a simple, low barrier, flip of a hydrogen from one side of the oxygen framework to the other. The pathway for this process is shown in Fig. 1. Extending this pathway one ultimately visits six equivalent minima through a cyclic process. All theoretical calculations performed thus far[16,20] indicate that this rearrangement process is a very facile one. Such low barrier rearrangement mechanisms naturally give rise to large ''tunneling'' splittings, and in fact the first treatments of torsion in the water trimer consider the motion as fast tunneling among the six equivalent minima on a one-dimensional potential energy surface.[17,18] In light of the understanding gained from the study of $(D_2O)_3$ and mixed isotope water trimers[2,5,26,27] it is perhaps more appropriate to consider such low barrier rearrangements as giving rise to a torsional (also termed ''pseudorotational'') vibrational energy level manifold resulting from the coupling of three degenerate torsional vibrations rather than as a genuine tunneling splitting. Experiments and theory on mixed isotope water trimers,[5,9,26,27] where the symmetry of the system is broken, confirm this analysis.

The permutation-inversion (PI) symmetry group associated with the torsional flipping between the six equivalent minima on the potential surface is the cyclic group G_6, isomorphic to the point group C_{3h}. The complex irreducible representations (irreps) of this group are conveniently labeled by the quantum number $k=0,\pm1,\pm2,3$ (modulo 6). A diagram showing the six lowest energy torsional vibrational levels of $(H_2O)_3$, along with the observed transitions, is given in Fig. 3. The corresponding frequencies calculated by van der Avoird *et al.*[6,7] with the *ab initio* potentials of Refs. 10 and 14 are listed in Table I. The symmetry of these levels has been compared to a Hückel treatment of the π electron system of benzene. The levels with $k=0$ and $k=3$ are nondegenerate, as are the A and B levels in benzene, while those with $k=\pm1$ and $k=\pm2$ are twofold degenerate, similarly to the benzene E levels. The energy increases with $|k|$, the

TABLE I. Experimentally determined torsional energy levels (in cm^{-1}) for the $(H_2O)_3$ and $(D_2O)_3$ isotopic forms of the water trimer, compared to the levels computed by fully coupled three-dimensional DVR calculations including the overall rotation of the trimer (Refs. 6 and 7). The computations were based on two torsional potential energy surfaces, DD pot. (Ref. 14) and BGLK pot. (Ref. 10).

	$(H_2O)_3$			$(D_2O)_3$		
k	Expt.	DD pot.	BGLK pot.	Expt.	DD pot.	BGLK pot.
0	0	0	0	0	0	0
±1	22.6979(2)	19.93	13.97	8.5385(1)	7.68	5.15
±2	65.6300(1)	59.07	44.15	27.9922(1)	25.18	17.15
3	87.0527(1)	81.23	62.33	41.0997(2)	36.62	24.73
3		161.01	143.85	90.3808(1)	96.15	88.93
±2		172.02	155.18	98.0991(1)	107.5	98.27

number of nodes in the real wave functions which for the degenerate levels are plus and minus combinations of the complex functions with $k=\pm1$ and $k=\pm2$. Transitions between these energy levels follow the selection rule

$$(k''-K'')-(k'-K')=3 \quad (\text{modulo } 6). \tag{1}$$

For the $k=0,\pm1,\pm2$ and 3 torsional levels observed in this work, this rule allows the permitted transitions to be easily determined, as well as the band polarization (parallel or perpendicular). The $k=3\leftarrow0$ transition at 87.1 cm^{-1}, for example, is only allowed for $\Delta K=0$, and hence is observed as a parallel band. The 65.6 cm^{-1} vibrational band is made up of two distinct perpendicular vibrational subbands, as $k=+2\leftarrow0$ is only allowed when $\Delta K=-1$ while $k=-2\leftarrow0$ is only allowed when $\Delta K=+1$. The third band, observed at 42.9 cm^{-1}, arises from the two parallel subbands $k=+2\leftarrow-1$ and $k=-2\leftarrow+1$. Coriolis effects perturb degenerate subbands severely, requiring us to treat each subband separately. It is perhaps more reasonable to think of the 42.9, 65.6, and 87.1 cm^{-1} torsional bands as transitions among six, rather than four, torsional energy levels.

Next we consider the bifurcation tunneling process shown in Fig. 2. This rearrangement mechanism, along with the ''flipping'' process discussed above, creates two distinct sets of 48 interconvertable equivalent minima on the water trimer potential energy surface and generates the molecular symmetry group for the water trimer, G_{48}. The group theory for these rearrangement processes has been examined extensively in a number of papers.[3,6,16] In order to understand the origins of the splittings in the newly observed bands, we must repeat some of the details here. The nondegenerate levels with $k=0$ and $k=3$ split into quartets with a constant and equal splitting (say β) between the individual components, which carry the $A_{1g}^{\pm}$, $T_u^{\pm}$, $T_g^{\pm}$, and $A_{1u}^{\pm}$ irreps of the group G_{48}. Including the overall rotation of the trimer, i.e., for nonzero J, the G_6 symmetry of the rovibrational states is determined by $k-K$. When K is not a multiple of 3 the G_{48} symmetries of the quartet components become more complicated, but the bifurcation splitting of the levels into equally spaced quartets remains basically intact. Because of the G_{48} selection rules each rovibrational transition between these nondegenerate levels is also split into a quartet. An experimental manifestation of such a splitting is shown, for example, in Fig. 4. The intensities of each quartet component nicely follow the nuclear spin statistics predicted for bifurcation tunneling in $(H_2O)_3$, namely a ratio of $A_{1u}:T_g:T_u:A_{1g}=11:9:3:1$ for rovibrational states with K a multiple of three and $\{A_{2u},A_{3u}\}:T_g:T_u:\{A_{2g},A_{3g}\}=8:9:3:0$ otherwise. The effect of the missing A_g symmetry components for states with $K\neq3n$ appear distinctly in the Q branch depicted in Fig. 4.

The degenerate torsional levels with $k=\pm1$ and $k=\pm2$ are split (for $J=0$) by bifurcation tunneling into six levels, carrying the $\{A_{2g}^{\pm},A_{3g}^{\pm}\}$ (degenerate), $T_u^{\pm}$ (twice), $T_g^{\pm}$ (twice), and $\{A_{2u}^{\pm},A_{3u}^{\pm}\}$ (degenerate) irreps of the group G_{48}. The splitting of these sextets is determined as follows. First, the levels split into the same type of equally spaced A_g, T_u, T_g, A_u bifurcation tunneling quartets as the nondegenerate $k=0$ and $k=3$ levels. The symbols A_g and A_u now represent the degenerate (complex conjugate) $\{A_{2g},A_{3g}\}$ and $\{A_{2u},A_{3u}\}$ states, respectively. In addition, there is a splitting between the two T_u components and between the two T_g levels, because these states of the same symmetry interact through the bifurcation tunneling process and repel each other. This was group theoretically derived in Ref. 6, and all the resulting bifurcation tunneling splittings of the levels were explicitly calculated in terms of two parameters β_2 and β_3, associated with two different possible bifurcation (donor) tunneling pathways (see Table II of Ref. 6). For the (constant) quartet splitting parameter β it was found that

$$\beta=\begin{cases}(2/3)(-2\beta_2-\beta_3) & \text{for } k=0\\ (2/3)(\beta_2+\beta_3) & \text{for } k=\pm1\\ (2/3)(\beta_2-\beta_3) & \text{for } k=\pm2\\ (2/3)(-2\beta_2+\beta_3) & \text{for } k=3.\end{cases} \tag{2}$$

The interaction matrix element between the $-|k|$ and $+|k|$ components of the same T_u or T_g symmetry is

$$\delta=\begin{cases}(2/3)(2\beta_2-\beta_3) & \text{for } k=\pm1\\ (2/3)(2\beta_2+\beta_3) & \text{for } k=\pm2.\end{cases} \tag{3}$$

For $J=0$ this interaction leads to a splitting of 2δ between these components. For $J>0$ this additional splitting between the two components of T_u symmetry and between those of T_g symmetry depends strongly on K, because the $-|k|$ and $+|k|$ substates are split by a Coriolis coupling term $\mp2\zeta CK$, linear in K (as explained below). For $K=0$ the $-|k|$ and $+|k|$ sublevels are in resonance and one finds the maximum splitting 2δ, just as for $J=0$. For $K\neq0$ the $-|k|$ sublevel is lowered by the linear Coriolis term, the $+|k|$

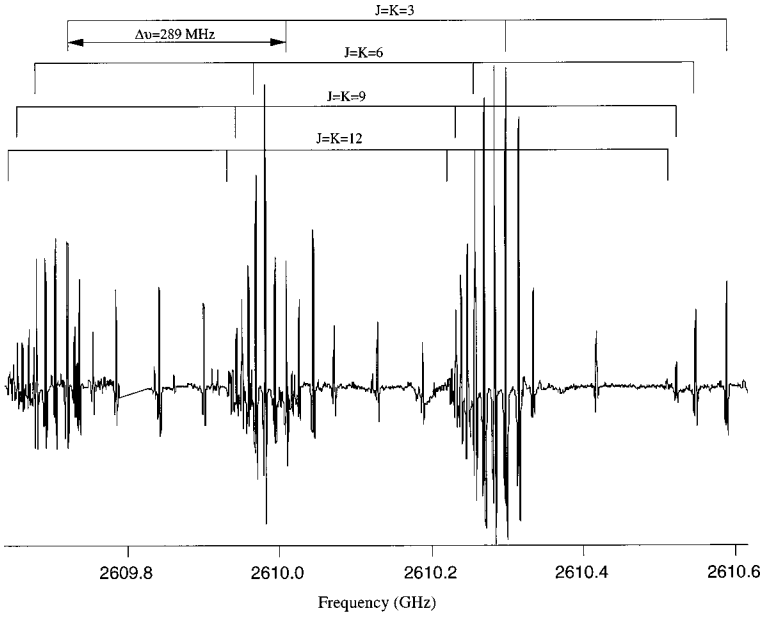

FIG. 4. Q branch of the 87.1 cm^{-1} torsional band. The quartet tunneling splitting is evident as four Q branches separated by a tunneling splitting of 289 MHz. Notice that the fourth component (A_g symmetry) has a nonzero nuclear spin weight only when K is a multiple of three. The relative intensities of the four components are not accurate due to long term drift in the laser power, as explained in the text.

sublevel is raised. Hence, the bifurcation (off-diagonal) coupling term δ becomes less effective, and the splitting between the pairs of T_u and T_g levels is strongly reduced. Especially for $(H_2O)_3$, where the Coriolis and bifurcation tunneling coupling matrix elements are of similar size, this leads to a complicated J,K dependent splitting pattern.

From here on we will globally indicate all the levels of G_{48} symmetries $A_{1g}, A_{2g}, A_{3g}, A_{1u}, A_{2u}, A_{3u}$ as A levels, sometimes distinguished into A_g and A_u, and those with T_u and T_g symmetries as T levels. Quantitative calculations of the torsional levels in Refs. 6 and 7, for $J=0$, 1, and 2, show that the splitting patterns indeed differ for the A levels and the T levels, cf. Figs. 2 and 3 in Ref. 6 and Tables III and IV in Ref. 7.

B. Effective rotational Hamiltonian

The techniques used in fitting the three vibrational bands (five subbands) in $(H_2O)_3$ correspond closely to those used in the corresponding global fit of $(D_2O)_3$ recently reported.[2] The analysis of the rotational structure in the torsional bands observed in $(D_2O)_3$ was achieved by derivation of an effective Hamiltonian, which takes into the account the Coriolis coupling between the large amplitude internal torsional motions and the overall rotation of the complex. This Hamiltonian was based on the explicit form of the rotational and Coriolis operators derived in Ref. 6. The effective Hamiltonian describing the rotational structure of each torsional level was obtained by second-order Van Vleck perturbation theory. For the nondegenerate torsional levels with $k=0$ and $k=3$ it simply reads as a standard symmetric rotor Hamiltonian

$$H_{\mathrm{eff}}^{\mathrm{rot}(k)} = B^{(k)} J^2 + [C^{(k)} - B^{(k)}] J_z^2 \tag{4}$$

with rotational constants $B^{(k)} = B + 2\mu_{+-}^{(k)}$ and $C^{(k)} = C + \mu_{zz}^{(k)}$ modified by the second-order Coriolis coupling parameters $\mu_{+-}^{(k)} = \mu_{-+}^{(k)}$ and $\mu_{zz}^{(k)}$, explicitly defined in Ref. 2.

For the degenerate torsional levels with $k=\pm 1$ and $k=\pm 2$ the situation is more complex because of the appearance of off-diagonal second-order Coriolis coupling matrix elements involving the shift operators J_+ and J_-. Partly these can be rewritten, with the use of the commutation relation

$$J_+ J_- - J_- J_+ = 2J_z, \tag{5}$$

and may then be taken into account as a diagonal Coriolis term, $\mp 2\zeta^{|k|} C^{|k|} J_z$, linear in J_z, with $-2\zeta^{|k|} C^{|k|}$ equal to the *second-order* Coriolis coupling matrix element $\mu_{+-}^{|k|} - \mu_{-+}^{|k|}$ defined in Ref. 2. This term has the same appearance as a standard *first-order* Coriolis term,[28] and its effects on the experimental spectra are very similar. The fact that it originates from second-order Coriolis coupling is related to the choice of the body-fixed frame in Ref. 6. Because of the large amplitude motions and the occurrence of tunneling between multiple equilibrium geometries in the water trimer, it is not possible to define such a frame by imposing the Eckart conditions that minimize the Coriolis coupling between internal motions and overall rotation. With the inclusion of all other, off-diagonal, coupling terms the effective rotational Hamiltonian for the levels with $k=\pm 1$ and $k=\pm 2$ becomes

$$\begin{aligned} H_{\mathrm{eff}}^{\mathrm{rot}(k',k)} = {} & \delta_{k',k}[B^{|k|} J^2 + (C^{|k|} - B^{|k|}) J_z^2 \mp 2\zeta^{|k|} C^{|k|} J_z] \\ & + \delta_{k',k-2(\mathrm{modulo}\ 6)} \mu_{--}^{(k)} J_- J_- \\ & + \delta_{k',k+2(\mathrm{modulo}\ 6)} \mu_{++}^{(k)} J_+ J_+ \end{aligned} \tag{6}$$

with the (modified) rotational constants $B^{|k|} = B + \mu_{+-}^{|k|} + \mu_{-+}^{|k|}$ and $C^{|k|} = C + \mu_{zz}^{|k|}$. All Coriolis coupling parameters

are defined in Ref. 2. For given J the matrix of this effective rotational Hamiltonian over the basis $|-|k|,K\rangle$ and $|+|k|,K\rangle$, with $K=-J,-J+1,\ldots,J$, has dimension $2(2J+1)$. It has nonzero elements only on the main diagonal and in the second codiagonal of the off-diagonal blocks between the substates with $k=-1$ and $k=+1$ and between those with $k=+2$ and $k=-2$, see Fig. 2 of Ref. 2. This matrix can simply be diagonalized (even analytically, in 2×2 blocks), for each value of J, to obtain the rovibrational levels and transition frequencies during the fit of the measured high resolution spectrum. Dramatic effects of both of these perturbations were also observed in the spectrum of $(H_2O)_3$.

C. Rotational and bifurcation tunneling structure in the levels of $(H_2O)_3$

The difficulty in assigning and fitting the $(H_2O)_3$ transitions was that of establishing a procedure to accurately describe the large splittings observed (described below) in each vibration. The magnitude of the bifurcation splitting in $(H_2O)_3$ is considerably ($\approx$60 times) larger than that observed in $(D_2O)_3$, putting the bifurcation tunneling splitting on the same scale as separations between rotational energy levels and making it necessary to include perturbations to the bifurcation tunneling splitting in the fit of the bands. In other words, there is strong interference between the effects of Coriolis coupling and of bifurcation tunneling, giving rise to strongly perturbed levels and spectra. The bifurcation tunneling splitting in $(D_2O)_3$ is small enough that any such perturbations are smaller than the accuracy of the fit ($\sim$2 MHz.). Hence, in the fit of the spectra of $(H_2O)_3$ we had to take into account the following effects, not included in $(D_2O)_3$.

In the nondegenerate torsional levels with $k=0$ and $k=3$ there is a small splitting of the levels with $K\neq0$, proportional to $J(J+1)$, which occurs only for the bifurcation levels of T symmetry, not for the A levels. The origin of this splitting was explained in Refs. 6 and 7; it is related to the additional splitting in the T levels of the degenerate ($k=\pm1$ and $k=\pm2$) states due to bifurcation tunneling, which we discussed above. This splitting, proportional to the bifurcation tunneling matrix element δ, also induces a splitting of the nondegenerate $k=0$ and $k=3$ levels by Coriolis mixing between the torsional eigenstates with $k=0$ and $k=\pm1$, and between those with $k=3$ and $k=\pm2$. The amount of Coriolis mixing is proportional to $\sqrt{J(J+1)}$, which leads to the $J(J+1)$ dependence of the level splittings. Since the Coriolis mixing conserves $k-K$ (modulo 6) one finds, in particular, that the basis function $|k=0, K=+1\rangle$ mixes with $|k=-1, K=0\rangle$, and that $|k=0, K=-1\rangle$ mixes with $|k=+1, K=0\rangle$, which induces a splitting of the $k=0$ level with $|K|=1$. Similarly, the basis function $|k=3, K=+1\rangle$ mixes with $|k=+2, K=0\rangle$, and $|k=3, K=-1\rangle$ with $|k=-2, K=0\rangle$, which causes the splitting of the $k=3$ level with $|K|=1$. Actually, these $|K|=1$ levels are the only ones where this ''Coriolis-induced bifurcation splitting'' is sufficiently large to be measurable. The bifurcation coupling between the functions $|k=-1, K=0\rangle$ and $|k=+1, K=0\rangle$ (of T_u and T_g symmetry) leads to a mixing of these functions with equal weights and, hence, of the functions $|k=0, K=+1\rangle$ and $|k=0, K=-1\rangle$ as well. Also the functions $|k=3, K=+1\rangle$ and $|k=3, K=-1\rangle$ are mixed into plus/minus combinations. Although the selection rule of Eq. (1) is still valid, these mixed states contain components with two different values of $k-K$, and the transitions between the split $k=0$ and $k=3$ levels involved in this mixing obey special selection rules.

These additional splittings of the levels with $k=0$ and $k=3$ were observed experimentally[7] in the $k=3\leftarrow0$ band at 87.1 cm^{-1}. Specifically, it was seen that only the P and R branches of the T lines are split, but not the Q branch, and that the splitting is proportional to J^2. This pattern is similar to the effects of ''axis switching'' in a nearly symmetric rotor. With the aid of the appropriate selection rules it could be deduced[7] that the bifurcation coupling parameter δ must be nearly of equal magnitude for $k=\pm1$ and $k=\pm2$, but differ in sign. From the expressions for δ given in Eq. (3), it then follows directly that $\beta_2\approx0$ and that bifurcation tunneling prefers the pathway corresponding to β_3. This pathway involves inversion of the complex, E^*.[16] From Eqs. (2) and (3) it also follows then that $|\delta|$ equals $|\beta|$ for both the levels with $k=\pm1$ and $k=\pm2$.

Also for the degenerate torsional levels with $k=\pm1$ and $k=\pm2$ we had to extend the theory. The bifurcation coupling (δ) between the level pairs of the same T_g or T_u symmetry, which we explained above, is roughly of the same size as the linear Coriolis coupling term in the effective rotational Hamiltonian. Hence, these effects interfere for $J>0$ and $K\neq0$, as discussed in Sec. II B, and the resulting line structure for the transitions involving these degenerate levels becomes very irregular. Since it is known from the theory in Ref. 6 that the bifurcation tunneling interaction between the $-|k|$ and $+|k|$ sublevels is diagonal in K, we solved this problem by simply adding, for the T levels, the term $\delta_{k',-k}\delta_{K',K}\delta$ to the effective rotational Hamiltonian of Eq. (6). In the matrix of the effective rotational Hamiltonian this gives rise to an additional (constant) term δ in all diagonal elements of the blocks that are off-diagonal in k. In Fig. 5 we show an example of such a matrix for $k=\pm1$ and $J=2$. Similar mixing occurs for the sublevels of T symmetry with $k=-2$ and $k=+2$, and we also include a constant δ on the diagonal of those blocks in the Hamilton matrix for $k=\pm2$ that are off-diagonal in k. This bifurcation matrix element δ may be taken as a parameter in the fit of the experimental spectra, just as the rotational and quartic distortion constants B, C, D_J, D_{JK}, D_K, the Coriolis constants ζ and $|\mu_{++}|$, and the bifurcation splitting constant β. Note, however, that these additional matrix elements δ occur only for the levels of T symmetry. They are absent for the A levels, and the structure of the Hamilton matrix used in the fit of these levels is the same as in Fig. 2 of Ref. 2. According to the theory, see Eqs. (2) and (3), combined with the observation (see the preceding paragraph) that the parameter β_2 is negligibly small, the bifurcation tunneling parameters β and δ of each band must be simply related: they are both equal to $(2/3)\beta_3$ in absolute value. We treated them as independent fit parameters and compare the results to the theory. Another relevant point is that it follows from the theory in Ref. 6 that both δ and μ_{++} are complex numbers. By a

$$
\begin{array}{c|ccccc|ccccc}
 & k=-1 & & & & & k=+1 & & & & \\
k=-1 & H^{(-1,-1)}_{-2,-2} & 0 & 0 & 0 & 0 & H^{(-1,1)}_{-2,-2} & 0 & H^{(-1,1)}_{-2,0} & 0 & 0 \\
 & 0 & H^{(-1,-1)}_{-1,-1} & 0 & 0 & 0 & 0 & H^{(-1,1)}_{-1,-1} & 0 & H^{(-1,1)}_{-1,1} & 0 \\
 & 0 & 0 & H^{(-1,-1)}_{0,0} & 0 & 0 & 0 & 0 & H^{(-1,1)}_{0,0} & 0 & H^{(-1,1)}_{0,2} \\
 & 0 & 0 & 0 & H^{(-1,-1)}_{1,1} & 0 & 0 & 0 & 0 & H^{(-1,1)}_{1,1} & 0 \\
 & 0 & 0 & 0 & 0 & H^{(-1,-1)}_{2,2} & 0 & 0 & 0 & 0 & H^{(-1,1)}_{2,2} \\
\hline
k=+1 & H^{(1,-1)}_{-2,-2} & 0 & 0 & 0 & 0 & H^{(1,1)}_{-2,-2} & 0 & 0 & 0 & 0 \\
 & 0 & H^{(1,-1)}_{-1,-1} & 0 & 0 & 0 & 0 & H^{(1,1)}_{-1,-1} & 0 & 0 & 0 \\
 & H^{(1,-1)}_{0,-2} & 0 & H^{(1,-1)}_{0,0} & 0 & 0 & 0 & 0 & H^{(1,1)}_{0,0} & 0 & 0 \\
 & 0 & H^{(1,-1)}_{1,-1} & 0 & H^{(1,-1)}_{1,1} & 0 & 0 & 0 & 0 & H^{(1,1)}_{1,1} & 0 \\
 & 0 & 0 & H^{(1,-1)}_{2,0} & 0 & H^{(1,-1)}_{2,2} & 0 & 0 & 0 & 0 & H^{(1,1)}_{2,2}
\end{array}
$$

FIG. 5. Effective rotational Hamiltonian matrix for a degenerate level with $k=\pm 1$ and $J=2$, with $K=-2,-1,0,1,2$. The diagonal elements are: $H^{(\pm 1,\pm 1)}_{K,K}=B^{(1)}J(J+1)+[C^{(1)}-B^{(1)}]K^2\mp 2\zeta^{(1)}C^{(1)}K$. In the off-diagonal blocks we have, on the diagonal: $H^{(1,-1)}_{K,K}=H^{(-1,1)}_{K,K}=\delta$ for the T levels, or $H^{(1,-1)}_{K,K}=H^{(-1,1)}_{K,K}=0$ for the A levels, and off-diagonal: $H^{(1,-1)}_{K+2,K}=H^{(-1,1)}_{K,K+2}=\mu^{(-1)}_{++}[J(J+1)-K(K+1)]^{1/2}[J(J+1)-(K+1)(K+2)]^{1/2}$.

simple basis transformation one can, however, obtain real values for these parameters (matrix elements). Hence, in the fit program we kept these fit parameters as real numbers, and diagonalized a real symmetric Hamilton matrix for each value of J to obtain the vibration–rotation–tunneling (VRT) levels.

At the end of this theory section, let us observe that we have checked the reliability of our effective rotational Hamiltonian by comparison of the energy levels obtained from the diagonalization of this Hamiltonian with the results of full calculations of the torsional levels for $J=0$, 1, 2, and 3. The latter include explicitly the coupled torsional motions by means of a three-dimensional discrete variable representation (DVR), as well as all Coriolis coupling effects, cf. Tables III and IV of Ref. 7 for $J\leqslant 2$. It turned out that our effective Hamiltonian gives an accurate representation of the level splittings and shifts from the full numerical computations, including the irregularities in the degenerate states with $k=\pm 1$ and $k=\pm 2$.

III. EXPERIMENT

The torsional bands of the H_2O water trimer discussed here have been measured over the past several years using the Berkeley terahertz laser spectrometers. The 87.1 cm^{-1} band was first reported[3] in 1994 by Liu *et al.* The 65.6 and 42.9 cm^{-1} bands are reported and analyzed here for the first time. The design of the spectrometers has been discussed previously,[29,30] and therefore only details relevant to these new bands are reported here. Briefly, a line-tunable 100 W CO_2 laser is used to pump a molecular gas terahertz laser, yielding a fixed frequency terahertz laser line. The laser lines used in this study include the 1193.7273 (CH_3OH), 1299.9954 (CH_3OD), 1397.1186 (CH_2F_2), 1891.2743 (CH_2F_2), 2058.1418 (CH_3OD), 2633.8991 ($^{13}CH_3OH$), and 2714.7151 GHz ($^{13}CH_3OH$) lasers. Tunability is achieved by mixing a fixed frequency laser line with microwave radiation on a Schottky barrier diode, a process that yields tunable sidebands of frequency $\nu_{\text{sidebands}}=\nu_{\text{laser}}\pm\nu_{\text{microwave}}$. A Martin–Puplett polarizing diplexer separates the tunable sidebands from the fixed frequency laser, after which the sidebands make 24 passes through a pulsed planar argon–water supersonic expansion[31] and are detected on a variety of terahertz detectors. The higher frequency 87.1 and 65.6 cm^{-1} bands were observed using a mechanically stressed Ge:Ga photoconductive detector while the 42.9 cm^{-1} band required the use of a Putley mode InSb hot electron bolometer. A brief description of the three $(H_2O)_3$ vibrational bands is given in Sec. IV.

IV. EXPERIMENTAL RESULTS

A. 87.1 cm^{-1} torsional band

The 87.1 cm^{-1} torsional band was the first observation of the $(H_2O)_3$ isotopic form of the water trimer. It is a textbook example of a parallel band of an oblate symmetric top and is remarkably unperturbed. It was measured in 1994 by Liu and co-workers using a planar cw expansion of argon and water and a multipass cell in the Perry configuration; this gave only eight passes of the laser through the throat of the expansion. This band is vastly more intense than both the 42.9 and 65.6 cm^{-1} bands, even when considering that the latter were measured with a pulsed slit expansion and a 24-pass Herriot cell.[32,33] As an example of the intensity exhibited by the 87.1 cm^{-1} band, the Q branch of the band has been detected through third-order mixing of the microwave radiation with the 118 μm laser.

Each rovibrational transition is split by bifurcation tunneling into the now familiar quartet depicted in Fig. 4. Each component of the quartet is separated from the other by a relatively constant 289 MHz, a slightly smaller splitting being observed at high values of the rotational quantum number J. The nuclear spin intensity ratios for the bifurcation pattern are 11:9:3:1 when $K=3n$ and 8:9:3:0 when $K\neq 3n$. Within the uncertainties imposed by laser power fluctuations the observed intensities of the quartet lines nicely match these ratios. The missing tunneling components when $K\neq 3n$ are clearly evident in the spectrum. One additional point worth noting is that each T state component arising from $|K|=1$ transitions is split into a doublet, a Coriolis effect explained by van der Avoird *et al.*[6,7] and in Sec. II C. We originally assigned this band to the torsional transition $k=3\leftarrow 0$, an assignment vindicated by the present analysis. The highest level torsional calculations[6,7] on the water trimer predict this 87.1 cm^{-1} band to occur at either 81.23 or 61.33 cm^{-1} depending on whether the DD or BGLK potential is used in the calculation respectively.

B. 65.6 cm^{-1} torsional band

More recently a perpendicular $(H_2O)_3$ spectrum was recorded near 66 cm^{-1}. That spectrum was assigned to the $k=\pm 2\leftarrow 0$ torsional transition based on the model calculations by van der Avoird *et al.* and on the ratio of the band origin to that of the corresponding $k=\pm 2\leftarrow 0$ transition in $(D_2O)_3$. The ratio of the $(H_2O)_3$ and $(D_2O)_3$ band origins

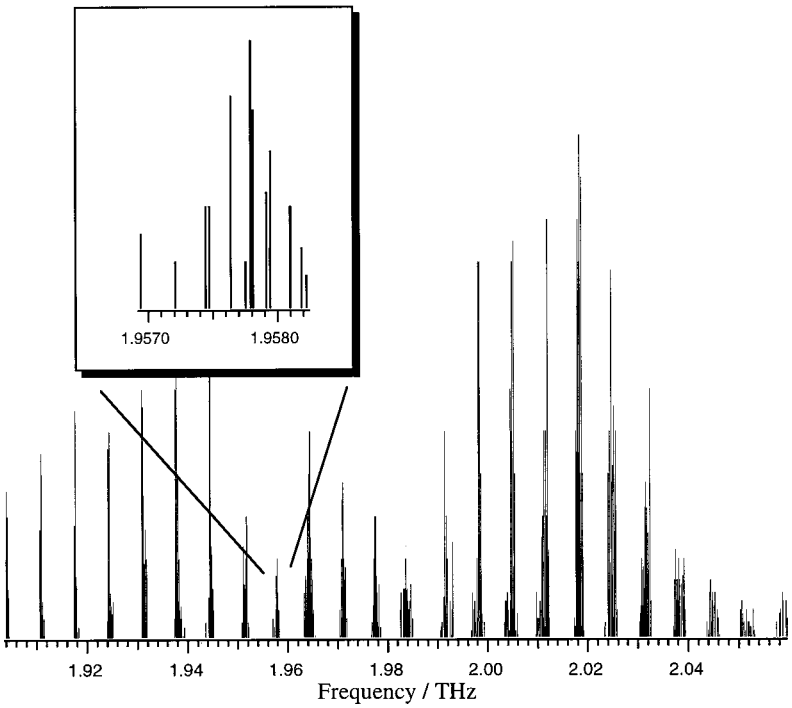

FIG. 6. Stick spectrum of the 65.6 cm^{-1} band, exhibiting the general features of a perpendicular band of a symmetric top. Note the perturbations evident in the $K=2\leftarrow1$ Q branch shown in the inset. A standard Q-branch progression, like that observed in the 87.1 cm^{-1} band, is not present.

for $k=\pm2\leftarrow0$ is 2.5 while the ratio for $k=3\leftarrow0$ is 2.1. Torsional calculations predict the newly observed band to arise at either 59.07 cm^{-1} (for the DD potential) or 44.15 cm^{-1} (for the BGLK potential) as shown in Table I.

This band was significantly weaker than the 87.1 cm^{-1} spectrum, even with the use of a pulsed supersonic slit jet and a 24-pass Herriot cell. A computer-assisted processing scheme was also used instead of boxcar averaging. The strongest transitions were observed with a signal to noise ratio of approximately 100/1.

Over 300 individual vibration–rotation–tunneling (VRT) transitions were recorded in a 5-cm^{-1}-wide region around the 65.6 cm^{-1} band origin. A plot of the strongest component of each tunneling quartet is shown in Fig. 6. Analogous to its deuterated counterpart, this $(H_2O)_3$ spectrum exhibits a variety of severe perturbations. The quartet spacing is not constant as a function of J and K, and both ''first-'' and second-order Coriolis perturbations similar to those observed in the D_2O trimer are also found.

An interesting feature of the bifurcation tunneling splittings not observed in the D_2O trimer spectra can be seen by close examination of the T tunneling components relative to the A components. A perturbation was observed that had not been evident in any of the previous water trimer bands. In the 65.6 cm^{-1} band the T_g and T_u states are separated by a constant 255 MHz, and the A_u and A_g components by a constant tunneling splitting of 765 MHz (3 times the 255 MHz spacing). However, it was noticed that the T components shift considerably relative to the A components, resulting in separations between the A and T components that vary from 200 to 300 MHz. This perturbation caused considerable difficulty in the rotational assignment of the band.

C. 42.9 cm^{-1} torsional band

Most recently we observed a parallel band of a symmetric top heavily perturbed by Coriolis effects near 43 cm^{-1}. It was therefore suspected to correspond to the $k=\pm2\leftarrow\pm1$ torsional transition, the only low frequency band of $(H_2O)_3$ expected to be both a parallel spectrum and strongly perturbed. The observation of this transition was a surprise, as the $k=\pm1$ torsional levels are 23 cm^{-1} above the ground state, suggesting that our expansion is not nearly as cold vibrationally as it is rotationally. The corresponding band in $(D_2O)_3$ has not been observed and is calculated[2] to lie close to 20 cm^{-1}, as can be seen in Table I. The perturbations in this band are particularly severe as both the $k=\pm2$ and the $k=\pm1$ torsional states are highly affected by Coriolis perturbations. Without the model Hamiltonian described in Sec. II it is unlikely that this band could have been fit to any reasonable degree.

Three terahertz lasers were used in the scanning of the 42.9 cm^{-1} band, the 1.193 727 3 THz laser of CH_3OH, the 1.299 995 4 THz laser of CH_3OD, and the 1.397 118 6 THz laser of CH_2F_2. The band is fairly weak, with the maximum signal to noise observed approximately 60/1. It was scanned using our most recent experimental setup, including a pulsed slit jet and computer-assisted processing scheme. A total of 137 transitions were assigned and fit, with J and K ranging from 0 to 20.

A stick-figure representation of the Q branch of the band is presented in Fig. 7. The two repelling Q branches are characteristic of a ''first-order'' Coriolis perturbation[28] and indeed, one of the perturbations in this band was modeled using a $\pm2\zeta CK$ term in the Hamiltonian. As a transition between two doubly degenerate levels, each of the perturbations discussed for the 65.6 cm^{-1} band is present in both the lower and upper state of the 42.9 cm^{-1} band. The large number of strong perturbations present in this band made the assignment of the rovibrational transitions a very difficult task.

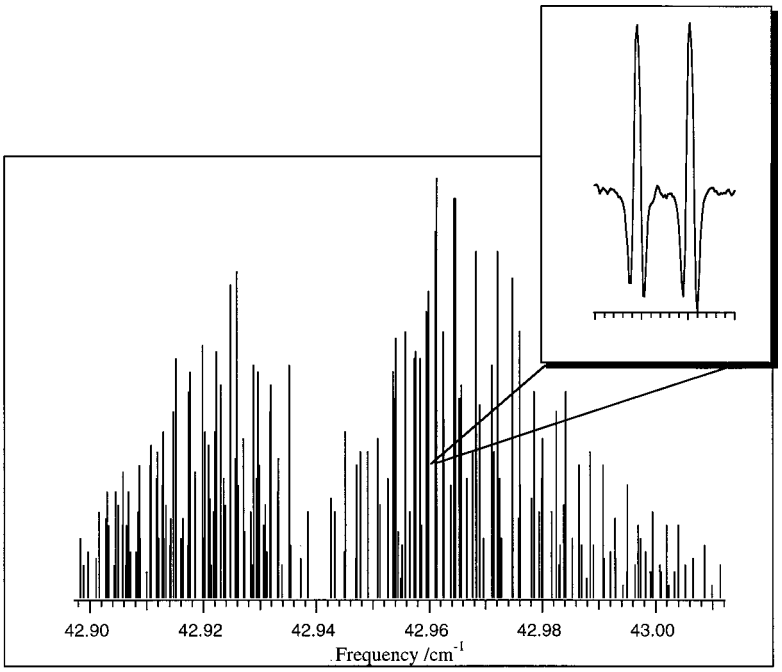

FIG. 7. The repelling Q branches of the 42.9 cm^{-1} band. The Q branch to the left is shifted to lower energy by the $-2\zeta CK$ pseudo-first-order Coriolis interaction, while the Q branch to the right is shifted to higher energy by $+2\zeta CK$. The inset shows a representative spectrum in a 10 MHz scan.

V. ANALYSIS OF THE TERAHERTZ SPECTRA

A. Global fit

The observed ordering of the symmetry components of the quartet in the 87.1 cm^{-1} band correspond to that expected for a quartet arising from a sum of tunneling splittings in the ground and excited states, as depicted in Fig. 8(a). All of the D_2O trimer torsional bands exhibit the opposite effect, viz. a quartet pattern that arises from a difference of tunneling splittings in the ground and excited states as shown in Fig. 8(b). It was found in the H_2O trimer that the central components of the bifurcation tunneling quartet (the T states) shift relative to the outer components (the A states), thus creating a quartet of transitions with an unequal spacing.

The global fit of the entire $(H_2O)_3$ VRT data set is presented on a band-by-band basis. In each band the A tunneling components are fit separately from the T tunneling components. Table II summarizes the optimized parameters (torsional energies, rotational and distortion constants, and Coriolis parameters) obtained from the final fit of the A states while Table III contains the parameters obtained from a fit of the T states. The overall result of the fit is a very precise description of the torsional vibrational levels of $(H_2O)_3$ up to energies of $\sim 150\ cm^{-1}$. A summary of the techniques used in fitting the A and T states is given below.

1. Bifurcation tunneling components of A symmetry

The A states of all three bands were fit using the method described in our paper on the global fit of the D_2O trimer torsional manifold.[2] The same two major classes of second-order Coriolis perturbations were observed, one acting like a diagonal ''first-order'' Coriolis perturbation ($\pm 2\zeta CK$) and the other an off-diagonal Coriolis perturbation represented by the Coriolis parameter $|\mu_{++}|$. The A_g states are separated from the A_u states by a constant amount, three times the tunneling splitting β reported for each band. In fact, the major difficulty in fitting the A states arose from assigning individual transitions embedded in dense and highly perturbed spectra. Once assigned, the model Hamiltonian derived in Ref. 2 and described in Sec. II B was highly effective for fitting the data. A summary of the optimized parameters obtained from the final fit of the A states is given in Table II.

2. Bifurcation tunneling components of T symmetry

Assigning and fitting the T bifurcation tunneling components was straightforward for the 87.1 cm^{-1} band, as it arises from a transition between two nondegenerate torsional vibrational levels, viz. $k=3\leftarrow 0$. A reasonably constant tunneling splitting of 289 MHz is observed, with slightly (~ 10 MHz) lower values recorded at the larger values of J.

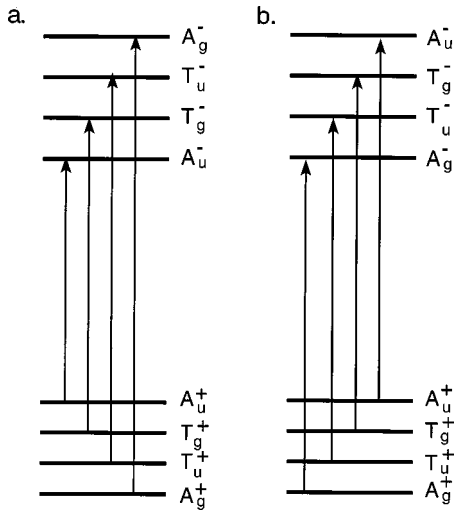

FIG. 8. The ordering of the bifurcation quartet in the excited state can give rise to observed tunneling splittings that are either the sum or the difference of splittings in the ground and excited torsional states. (a) An example of a sum of tunneling splittings, as observed in the 87.1 and 65.6 cm^{-1} bands. (b) An example of a difference of tunneling splittings, as observed in the 42.9 cm^{-1} band and all $(D_2O)_3$ trimer torsional bands.

TABLE II. Parameters (in megahertz, except ζ which is dimensionless) obtained by a fit of 361 $(H_2O)_3$ bifurcation tunneling states of A symmetry to the model torsional Hamiltonian derived here. E_0 is the torsional vibrational energy, A, B, C, D_J, D_{JK}, and D_K are rotational and distortion constants, and ζ and μ_{++} are Coriolis perturbation parameters. The three C constants could not be determined independently and therefore the ground state C was fixed at 3513.98 MHz as explained in the text.

	$k=0$	$k=+1$	$k=-1$	$k=+2$	$k=-2$	$k=3$
E_0	0.0[a]	680 605.3(4)		1 967 970.0(3)		2 609 774.9(2)
$B(=A)$	6646.91 (2)	6 641.73(4)		6 632.11(2)		6 626.10(2)
C	3513.98[a]	3 516.35(2)		3 518.07(2)		3 514.77(1)
D_J	0.0417(2)	0.041(1)	0.0413(9)	0.0410(5)	0.0404(4)	0.0405(3)
D_{JK}	−0.0631(6)	−0.064(3)	−0.064(2)	−0.063(2)	−0.062(1)	−0.0627(8)
D_K	0.027(2)	0.030(3)	0.028(2)	0.028(3)	0.027(2)	0.027(2)
ζ	0.0	−0.053 02(2)		−0.039 50(1)		0.0
$\lvert\mu_{++}\rvert$	0.0	15.344(2)		17.47(1)		0.0

[a]Value fixed to avoid correlation.

The sole perturbation recorded is a small symmetrical splitting of rovibrational transitions with $|K|=1$, observed only in the P and R branches of the band. This splitting has been previously explained,[6,7] see Sec. II C.

Fitting the T bifurcation tunneling components for transitions involving degenerate vibrational levels required considerably more effort. Each degenerate vibrational level included in the T state fit required the diagonalization of a different, slightly more complex Hamiltonian matrix than that used for the A states. An example of the matrix used in the fit of the $J=2$ energy levels of the 65.6 cm^{-1} band is shown in Fig. 5. Note that the extra perturbation term δ requires us to diagonalize the matrix in order to determine the energy levels. No simple analytical solution exists, as was the case for the A components and in our fit of the torsional manifold of $(D_2O)_3$. Fortunately, it was found to be possible to assign the eigenvalues of the matrix to particular rotational states. The energy separation between different values of K is sufficient to distinguish the eigenvalues and allow assignment to specific J and K quantum numbers. It is possible to consider the addition of the parameter δ as a perturbation on the ''normal'' analytical solutions derived for both $(D_2O)_3$ and the A states of $(H_2O)_3$ while assigning transitions.

Diagonalizing the matrix in Fig. 5 splits nearly all of the degeneracies that would be present in a normal symmetric top in a degenerate vibrational level. The majority of these splittings are small (a few megahertz) with a few notable exceptions. The largest of these exceptions arises in states pushed to higher energy by the ''first-order'' Coriolis term $+2\zeta CK$ with $K=1$. This reasonably large splitting is also observed in the A states and in the D_2O trimer and is a standard result of the analytical solution of the A state Hamiltonian matrix (without the extra coupling term δ). The magnitude of this splitting varies considerably with J and K but is approximately a few hundred megahertz. The smaller predicted splittings arise directly from the T state coupling term δ, and are therefore only seen in the T states. The largest of these splittings arises in states with $K=0$. This splitting is equal to 2δ and is a direct prediction from the diagonalization of the matrix in Fig. 5. It is seen distinctly in both the 65.6 and 42.9 cm^{-1} bands. Smaller splittings of up to a few megahertz are predicted in other rovibrational levels. None of these smallest splittings are observed.

A final and unexpected perturbation noticed in the bifurcation tunneling states of $(H_2O)_3$ was a shift of the T states relative to the A states. The simplest example of this perturbation arises in the 65.6 cm^{-1} band, as the perturbation is only observed in the excited state in that transition. In the 65.6 cm^{-1} band the separation between the T_g and the T_u tunneling components is a constant 255 MHz, exactly the value for the tunneling splitting derived from the splitting between the A states. The two T components, however, shift relative to the A states, creating an unequal bifurcation tunneling splitting. The magnitude of this shift is plotted in Fig. 9 for the 65.6 cm^{-1} band, which shows the separation between the A_u state (the lowest energy bifurcation tunneling component) and T_g, the lowest energy T state. States pushed to higher frequency by the diagonal Coriolis term $+2\zeta CK$ have a larger separation between the first two bifurcation tunneling components while states pushed to lower frequency by the Coriolis term $-2\zeta CK$ have a smaller separation.

It should be noted that the dynamics of the bifurcation tunneling process have not yet been treated by theory, only a qualitative group theoretical treatment and a simple param-

TABLE III. The T bifurcation tunneling components of $(H_2O)_3$ were observed to shift relative to the A components by an amount that is exponentially dependent on the rotational quantum number K. This exponential shift is given by the parameters a, b (in megahertz) and c according to the formula: shift$=a+b\exp(-cK)$. The energy of the T_u state can be calculated from the energy of the corresponding A_g state, found from the parameters in Table II, by adding a constant β and the appropriate exponential shift to the energy of this A_g state. The addition of another constant β gives the energy of the T_g state. This gives an accurate determination of the T state energy levels (with errors are less than 2 MHz). The bifurcation tunneling parameters β and δ are defined in the text, see Eqs. (2) and (3).

	$k=-1$	$k=+1$	$k=-2$	$k=+2$
a	−8.3551	5.9747	−15.496	16.863
b	−137.7	129.55	−115.01	113.5
c	0.21881	0.200 77	0.404 38	0.405 54
$\lvert\delta\rvert$	147 MHz		119 MHz	
$\lvert\beta\rvert$	$\lvert\beta(k=0)\rvert+\lvert\beta(k=3)\rvert=289.0$ MHz $\lvert\beta(k=0)\rvert+\lvert\beta(k=\pm2)\rvert=253.46$ MHz $\lvert\beta(k=\pm2)\rvert-\lvert\beta(k=\pm1)\rvert=38.88$ MHz			

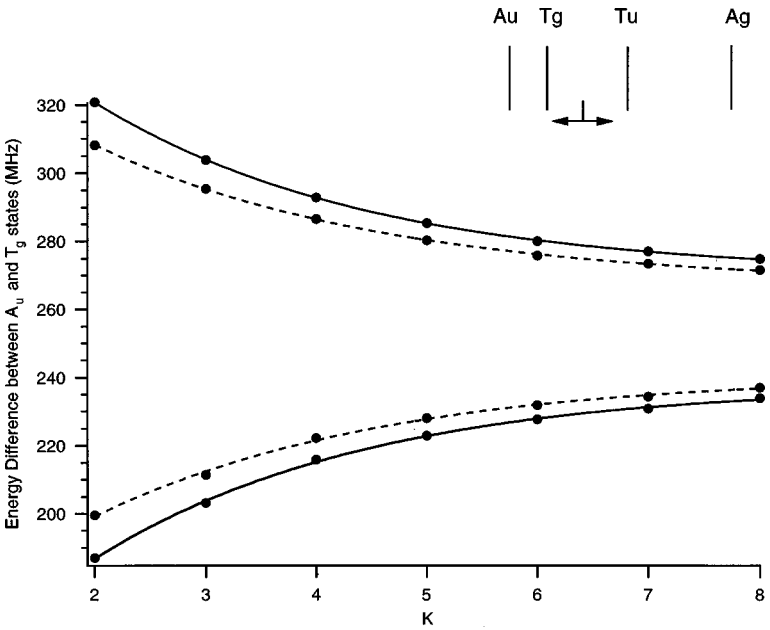

FIG. 9. Exponential shift of the T_g and T_u tunneling components relative to the A_u and A_g components, shown here for the 65.6 cm^{-1} band. The splitting between T_g and T_u remains a constant 255 MHz but the two T states shift relative to the A_u and A_g components. The dotted line in the spectrum is the actual frequency difference between the A_u and T_g tunneling components. The solid line is the shift after correction for the small frequency shifts predicted for the T states by the inclusion of the parameter δ.

etrized model were given in Refs. 6 and 7. We therefore do not know whether the bifurcation tunneling splitting ''constants'' β and δ actually depend on J and/or K. As can be seen in Fig. 9 the shift of the T states with respect to the A states changes exponentially with K. Note, however, that the exponentials in Fig. 9 do not converge to 255 MHz as would be expected from the constant tunneling splitting between the A_u and A_g states. Interestingly, the lower exponential converges to 238 MHz while the higher exponential converges to 272 MHz, equally spaced around the 255 MHz tunneling splitting. Perhaps this indicates that there is yet another small (a few megahertz) perturbation shifting the T states by a constant amount, and combining with the exponential shift to give us the spectrum we observe.

B. 87.1 cm^{-1} torsional band

The 87.1 cm^{-1} parallel torsional band was fit by Liu *et al.* to the standard symmetric rotor energy level expression

$$E_{J,K}=E_0+BJ(J+1)+(C-B)K^2-D_JJ^2(J+1)^2 - D_{JK}J(J+1)K^2-D_KK^4, \quad (7)$$

where E_0 is the vibrational energy of the torsional state, B and C are the rotational constants, and D_J, D_{JK}, and D_K are the quartic distortion constants. Liu reported that Eq. (7) gave a very high quality fit of the observed transitions. This observation is in agreement with the theory in Ref. 2 and in Sec. II, cf. Eq. (4) for the nondegenerate torsional energy levels with $k=0$ and $k=3$. The quartic distortion terms in Eq. (7) represent the higher-than-second-order Coriolis effects, not yet included in the theory that leads to Eq. (4). The band was therefore fit as a normal symmetric top with each tunneling component separated by a constant 289 MHz. In the P and R branches the splitting gets slightly smaller at higher values of J ($\sim$10 MHz smaller at $J=5$). No significant deviation from the 289 MHz splitting was observed for the Q branch. From the fit of this vibration the rotational constants for the $k=0$ and $k=3$ torsional levels were derived, with the exception of the C rotational constant. It is well known that a parallel ($\Delta K=0$) vibrational band does not allow independent determination of the ground and excited state C constants, only their difference (ΔC).

The only Coriolis perturbation evident in the 87.1 cm^{-1} band was a small splitting of the T state components of all $K=1$ transitions in the P and R branches. This splitting increases proportionally to J^2 [not $J(J+1)$]. The origin of this splitting, a Coriolis-induced bifurcation splitting, was explained in detail in Sec. II C, and the J^2 dependence in Refs. 6 and 7. This splitting is also observed in the 65.6 cm^{-1} torsional band in all subbands, the P, Q, and R branches of both the $\Delta K=+1$ and the $\Delta K=-1$ subbands. The small splitting is predicted to occur only in nondegenerate torsional levels and, in agreement with this prediction, it is not observed in the 42.9 cm^{-1} band.

A total of 112 A state transitions were included in the fit of the 87.1 cm^{-1} band, with J and K values ranging from 0 to 11.

C. 65.6 cm^{-1} torsional band

The other vibrational band originating from the torsional ground state, the 65.6 cm^{-1} band, is assigned to the perpendicular torsional transition $k=\pm2\leftarrow0$. A total of 107 transitions were added to the global fit with the assignment of the A states of this transition, including values of J and K ranging from 0 to 13. The fit of the A states of this band was accomplished as described in our paper on $(D_2O)_3$. Normally, fitting a perpendicular band of a symmetric top would allow us to independently determine the vibrationally averaged C rotational constants for both the ground and excited state. Unfortunately, as noticed in the global fit of the $(D_2O)_3$ torsional transitions, the diagonal Coriolis term $\pm2\zeta CK$ cannot be uncoupled from the C rotational constant. In the D_2O trimer this was dealt with by fixing the value of the ground state C constant to approximately the value published by Liu *et al.*[3] in his fit of the 98.1 cm^{-1} of

$(D_2O)_3$. In the H_2O trimer we have arbitrarily fixed the ground state C constant at a value that gives the same inertial defect as that previously published for the D_2O trimer.

All of the Coriolis perturbations that have been discussed thus far strongly affect the 65.6 cm^{-1} band. Once the individual rovibrational transitions were assigned, the A state transitions were not difficult to include in the fit as the model Hamiltonian derived for the D_2O trimer describes the A states of the H_2O trimer exceedingly well. The T state transitions were a considerably more difficult problem. The model Hamiltonian for the T states derived in Sec. II C of this paper was used for an initial fit. All parameters except δ were held at the same values found for the A states. If the bifurcation tunneling splitting had been a constant value as in the 87.1 cm^{-1} band, this method would have given a precise description of the T state transitions. It was found, however, that the bifurcation tunneling did not give rise to equally spaced quartets. The T states are shifted with respect to the A states as described earlier. The final fit parameters for the A bifurcation tunneling components are reported in Table II while the fit parameters for the T states are reported in Table III. Note that we used two sets of quartic distortion constants, one set for the sublevels with $k=+2$ and and one for $k=-2$, since the effects of the higher order Coriolis interactions represented by these distortion constants are not explicitly included in the theory that led to our effective rotational Hamiltonian. However, the values obtained from the fit to the experimental spectrum are quite similar for the two sublevels, see Table II.

D. 42.9 cm^{-1} torsional band

The 42.9 cm^{-1} band is assigned to the torsional transition $k=\pm 2 \leftarrow \pm 1$. The observation of this transition allowed us to complete the torsional manifold shown in Fig. 3. Assigning the A states of the band was straightforward. The tails of the Q branch were examined and progressions between the most intense lines were followed into the heart of the band. These reasonably intense progressions were assigned as $J=K$ transitions. Progressions in the P and R branches were then added to the fit, locking in many of the fit parameters.

The assignment of the T states also began in the tails of the Q branches. Progressions found among unassigned lines were assumed to arise from T state transitions. A constant 39 MHz tunneling splitting between the T states (the central two components of the bifurcation tunneling quartet) was determined and a full assignment quickly resulted. This 39 MHz spacing represents a difference between the tunneling splitting in the $k=\pm 2$ and $k=\pm 1$ torsional states as described previously. A total of 363 components were fit representing 137 rovibrational transitions.

Finally, let us discuss the relation between the values of β and δ extracted from the experimental spectra, see Table III. It is predicted by the above-mentioned theory that $|\beta| = |\delta|$ for each of the degenerate torsional levels with $k=\pm 1$ and $k=\pm 2$. Crudely, it can be concluded from the data in Table III that this is indeed the case, and that the values of $|\beta|$ and $|\delta|$ for all the (lower) torsional levels are about 135 ± 20 MHz. However, if one tries to extract more precise values of the individual $|\beta|$'s from these data, one seems to reach the limits of the simple theoretical picture that we used for the bifurcation tunneling process. Also the observed J,K dependence of the bifurcation splitting parameter β and the (K-dependent) shift between the A levels and T levels indicate that our simple treatment of bifurcation tunneling should be refined in order to reproduce all the spectroscopically measured details.

VI. CONCLUSIONS

We report a global fit of all the VRT data existing for the H_2O water trimer in the terahertz region. This effects a precise experimental determination of the lowest six torsional sublevels of $(H_2O)_3$. The quality of the fit is reflected in the rms deviation of 0.93 MHz, less than the typical experimental error of 2 MHz. Correlations as high as 0.99 between several distortion constants and rotational constants B'' and B' were observed; most parameters were relatively uncorrelated, however.

We recently reported the determination of a spectroscopic pair potential for the water dimer.[19] The existence of such a highly accurate pair potential will make it possible to consider the analysis of the complicated multibody forces present in larger water clusters, specifically the three-body forces. In time it seems likely that it will be possible to fit the multibody forces in the water trimer to the spectra reported here through adjustment of the parameters of specific three-body terms added to an accurate pair potential, as was accomplished for the multibody forces in the simpler Ar_2HCl and Ar_2DCl clusters.[34] In this stepwise fashion, an accurate description of the force field of the bulk phases of water may ultimately be obtained. An alternative approach to this problem is the use of advanced *ab initio* electronic structure methods to compute accurate pair and three-body potential surfaces for water. Such potentials have recently been obtained and used in quantum calculations of the energy levels associated with the internal (tunneling and vibrational) motions in the water dimer and trimer.[35] By comparison with detailed spectroscopic data it is possible to establish their accuracy and, if necessary, to improve them. Considerable progress has also been made in this direction. It is this goal that has motivated our efforts toward a completely assigned and analyzed data set for the water trimer.

This work completes a large body of work on the torsional dynamics of the $(D_2O)_3$, $(H_2O)_3$, and mixed isotope forms of the water trimer below 150 cm^{-1}. The observation of several mixed isotope water trimer transitions at similar frequencies to pure water trimer transitions suggested that the torsional dynamics in the water trimer should properly be treated as a vibration, rather than as a pure tunneling problem. Recent theoretical work on these systems is in agreement with this analysis.[5] Recently we reported the characterization of the torsional dynamics of $(D_2O)_3$ through a high quality global fit of the lowest five torsional bands (nine subbands) to a parametrized energy level expression obtained using second-order perturbation theory on a model Hamiltonian. Perhaps the most interesting and unexpected

feature of this fit of the torsional energy levels of $(H_2O)_3$ and $(D_2O)_3$ was that second-order perturbation theory on a model Hamiltonian including only spatial rotation of the cluster and the three torsional degrees of freedom, out of the total of 21 vibrational degrees of freedom, could give such very high quality results. This implies that an adiabatic separation of the torsional coordinates from the other, higher frequency, intra- and intermolecular vibrational modes yields a good approximation in the treatment of the torsional manifold of the water trimer. The bifurcation tunneling dynamics, treated group theoretically here, remain to be characterized in terms of the associated potential energy surface. The bifurcation tunneling splittings observed, however, may be accurately described through the simple addition of an exponential dependence on the rotational quantum number K to the rovibrational energy level expression. The combination of experimental and theoretical work on $(H_2O)_3$, $(D_2O)_3$, and mixed isotope water clusters thus provides an excellent description of the torsional and bifurcation dynamics in the water trimer.

ACKNOWLEDGMENTS

This work was supported by the Experimental Physical Chemistry Program of the US National Science Foundation. A.v.d.A. thanks Dr. Paul E. S. Wormer for critically reading the manuscript.

[1] N. Pugliano and R. J. Saykally, Science **257**, 1937 (1992).
[2] M. R. Viant, M. G. Brown, J. D. Cruzan, R. J. Saykally, M. Geleijns, and A. van der Avoird, J. Chem. Phys. **110**, 4369 (1999).
[3] K. Liu, J. G. Loeser, M. J. Elrod, B. C. Host, J. A. Rzepiela, N. Pugliano, and R. J. Saykally, J. Am. Chem. Soc. **116**, 3507 (1994).
[4] K. Liu, M. J. Elrod, J. G. Loeser, J. D. Cruzan, N. Pugliano, M. G. Brown, J. Rzepiela, and R. J. Saykally, Faraday Discuss. **35**, 34 (1994).
[5] M. Geleijns and A. van der Avoird, J. Chem. Phys. **110**, 823 (1999).
[6] A. van der Avoird, E. H. T. Olthof, and P. E. S. Wormer, J. Chem. Phys. **105**, 8034 (1996).
[7] E. H. T. Olthof, A. van der Avoird, P. E. S. Wormer, K. Liu, and R. J. Saykally, J. Chem. Phys. **105**, 8051 (1996).
[8] J. M. Sorenson, J. K. Gregory, and D. C. Clary, Chem. Phys. Lett. **263**, 680 (1996).
[9] D. Sabo, Z. Bacic, S. Graf, and S. Leutwyler, Chem. Phys. Lett. **261**, 318 (1996).
[10] T. Burgi, S. Graf, S. Leutwyler, and W. Klopper, J. Chem. Phys. **103**, 1077 (1995).
[11] W. Klopper, M. Schutz, H. P. Luthi, and S. Leutwyler, J. Chem. Phys. **103**, 1085 (1995).
[12] W. Klopper and M. Schutz, Chem. Phys. Lett. **237**, 536 (1995).
[13] D. Sabo, Z. Bacic, T. Burgi, and S. Leutwyler, Chem. Phys. Lett. **244**, 283 (1995).
[14] J. G. C. M. van Duijneveldt-van de Rijdt and F. B. van Duijneveldt, Chem. Phys. Lett. **237**, 560 (1995).
[15] J. K. Gregory and D. C. Clary, J. Chem. Phys. **102**, 7817 (1995).
[16] D. J. Wales, J. Am. Chem. Soc. **115**, 11180 (1993).
[17] M. Schutz, T. Burgi, S. Leutwyler, and H. B. Burgi, J. Chem. Phys. **99**, 5228 (1993).
[18] M. Schutz, T. Burgi, S. Leutwyler, and H. B. Burgi, J. Chem. Phys. **100**, 1780 (1994).
[19] R. S. Fellers, L. B. Braly, M. G. Brown, C. Leforestier, and R. J. Saykally, Science **284**, 945 (1999).
[20] J. E. Fowler and H. F. Schaefer, J. Am. Chem. Soc. **117**, 446 (1995).
[21] S. S. Xantheas and T. H. Dunning, Jr., J. Chem. Phys. **98**, 8037 (1993).
[22] S. S. Xantheas and T. H. Dunning, Jr., J. Chem. Phys. **99**, 8774 (1993).
[23] G. Chalasinski, M. M. Szczesniak, P. Cieplak, and S. Scheiner, J. Chem. Phys. **94**, 2873 (1991).
[24] J. C. Owicki, L. L. Shipman, and H. A. Scheraga, J. Phys. Chem. **79**, 1794 (1975).
[25] T. R. Walsh and D. J. Wales, J. Chem. Soc., Faraday Trans. **92**, 2505 (1996).
[26] K. Liu, M. G. Brown, M. R. Viant, J. D. Cruzan, and R. J. Saykally, Mol. Phys. **89**, 1373 (1996).
[27] M. R. Viant, J. D. Cruzan, D. D. Lucas, M. G. Brown, K. Liu, and R. J. Saykally, J. Phys. Chem. A **101**, 9032 (1997).
[28] G. Herzberg, *Infrared and Raman spectra of Polyatomic Molecules* (Van Nostrand, New York, 1945).
[29] G. A. Blake, K. B. Laughlin, R. C. Cohen, K. L. Busarow, D. H. Gwo, C. A. Schmuttenmaer, D. W. Steyert, and R. J. Saykally, Rev. Sci. Instrum. **62**, 1693 (1991).
[30] G. A. Blake, K. B. Laughlin, R. C. Cohen, K. L. Busarow, D. H. Gwo, C. A. Schmuttenmaer, D. W. Steyert, and R. J. Saykally, Rev. Sci. Instrum. **62**, 1701 (1991).
[31] K. Liu, R. S. Fellers, M. R. Viant, R. P. McLaughlin, M. G. Brown, and R. J. Saykally, Rev. Sci. Instrum. **67**, 410 (1996).
[32] D. R. Herriott, H. Kogelnik, and R. Kompfner, Appl. Opt. **3**, 523 (1964).
[33] D. R. Herriott and H. J. Schulte, Appl. Opt. **4**, 883 (1965).
[34] M. J. Elrod and R. J. Saykally, Chem. Rev. **94**, 1975 (1994).
[35] G. C. Groenenboom, E. M. Mas, R. Bukowski, K. Szalewicz, P. E. S. Wormer, and A. van der Avoird (unpublished).
[36] K. Liu, K. , M. G. Brown, C. Carter, R. J. Saykally, J. K. Gregory, and D. C. Clary, Nature (London) **381**, 501 (1996).